

Article

Not peer-reviewed version

Viscosity Analysis of Electron-Beam Degraded Gellan in Dilute Aqueous Solution

Fathi Elashhab , Lobna Sheha , [Nada Elzawi](#) ^{*} , [Abdelsallam EA. Youssef](#)

Posted Date: 30 July 2025

doi: 10.20944/preprints202507.2548.v1

Keywords: e-beam degradation; gellan intrinsic viscosity; scaling laws; chain flexibility; activation functions



Preprints.org is a free multidisciplinary platform providing preprint service that is dedicated to making early versions of research outputs permanently available and citable. Preprints posted at Preprints.org appear in Web of Science, Crossref, Google Scholar, Scilit, Europe PMC.

Copyright: This open access article is published under a Creative Commons CC BY 4.0 license, which permit the free download, distribution, and reuse, provided that the author and preprint are cited in any reuse.

Article

Viscosity Analysis of Electron-Beam Degraded Gellan in Dilute Aqueous Solution

Fathi Elashhab, Lobna Sheha, Nada ELzawi * and Abdelsallam EA. Youssef

Chemistry Department, Faculty of Science, University of Benghazi

* Correspondence: nada.elzawi@uob.edu.ly

Abstract

This study explores the effect of E-beam radiation on gellan conformations in dilute aqueous solutions. Native and E-beam-modified gellan samples (N&EBMs) were prepared at 0.05 g/cm³ in 0.1M KCl under atmospheric conditions. Their relative viscosities were measured at different temperatures, and intrinsic viscosity and molar mass were determined using the Solomon–Ciuta and Mark-Houwink equations. The degradation of molar mass was analyzed, and first-order rate constants and degradation lifetimes were calculated. Structural properties such as the radius of gyration and second virial coefficient were evaluated, yielding scaling coefficients of 0.62 and 0.15, respectively, indicating that gellan chains adopt a perturbed coil structure in a good solvent. The shape parameter confirmed that E-beam radiation did not affect the ideal random coil structure of gellan. Chain flexibility was assessed using theoretical models, including the transition state theory (TST), freely rotating chain (FRC) model, and worm-like chain (WLC) model. According to TST, E-beam radiation reduced molar mass and activation energy while increasing activation entropy, decreasing chain flexibility but enhancing solvent quality. FRC model provided the end-to-end distance (R_0) and characteristic ratio (C_∞), while WLC model determined the persistence length (l_p). E-beam radiation decreased R_0 and increased l_p , suggesting reduced flexibility and improved solvent interactions. However, C_∞ remained largely unchanged, indicating that gellan retained its ideal chain structure despite radiation exposure. These findings offer insight into the structural and conformational changes in gellan under E-beam radiation, with implications for its rheological and functional properties.

Keywords: e-beam degradation; gellan intrinsic viscosity; scaling laws; chain flexibility; activation functions

1. Introduction

Polymers are distinctive materials characterized by a wide range of high molar masses and corresponding solution viscosities [1]. They are composed of chain molecules formed by repeating organic units called monomers, where each pair of monomers is covalently bonded [2].

In solution, the length of the covalent bond (b) is usually referred to as the chain segment; the length of a single polymer chain corresponds to a specific number of segments (N) and degree of polymerization (DP), where N is equal to $2 DP$; the degree of polymerization, also called the number of monomers, is equal to the chain molar mass (M) divided by the monomer molar mass M_u [1]. Both are represent average values due to the varying chain lengths of polymeric substances.

In a diluted solution, polymer chains exist as individual coils and behave either as a random walk coils or self-avoiding walk coils [3–5]. In a good solvent, these coils adopt irregular and dynamic shapes due to segmental perturbations, behaving like a real chain that is fully dissolved and conforming to the self-avoiding walk (SAW) model [4,5]. However, electrolyte chains tend to adopt stretched conformations unless a small amount of neutralizing salt is added, which causes the chains to collapse back into the coil shapes [1].

In contrast, in a theta (θ) solvent, the coil assumes a static, spherical shape due to its unperturbed segments, following the random walk (RW) model or freely rotating chain (FRC) model [3–5]. In this case, the chain behaves like an ideal chain, neither completely dissolved nor precipitate.

Polymers in infinitely diluted solutions (IDS) exhibit specific intrinsic properties (P_s) such as intrinsic viscosity ($[\eta]$), radius of gyration (R_g), chain end-to-end distance (R_e), hydrodynamic radius (R_h), and interaction parameter (A_2). Their relationships play a critical role in the viscosity analysis of polymers in solution [1,4–7].

Polysaccharides are natural polymer, composed of glycosidic-linked mono-saccharide units, and commonly utilized in numerous industrial and biomedical contexts [8]. A key task in these applications is controlling the M - P relationships of polysaccharides. Radiation degradation methods, such as electron beam (EB) techniques, are effective, eco-friendly ways to regulate these relationships. When irradiated polysaccharides are dissolved in a solution, their viscosity behavior often differs from that of the native polysaccharides, see for example Ref. [9–12].

In dilute solutions, polysaccharides exhibit a range of M - P relationships, which are typically analyzed Flory [4,13] scaling laws and theoretical models such as the FRC and SAW models, as previously discussed [3–5]. Additionally, the transition state theory (TST) and the worm-like chain (W-LC) model, covered in References [6,14] and [1,8,15], provide further insight into their behavior.

Gellan is a linear, water-soluble polysaccharide obtained through bacterial fermentation [15,16]. It functions as an anionic polysaccharide and is composed of repeating monomeric units, as shown in Figure 1 [16].

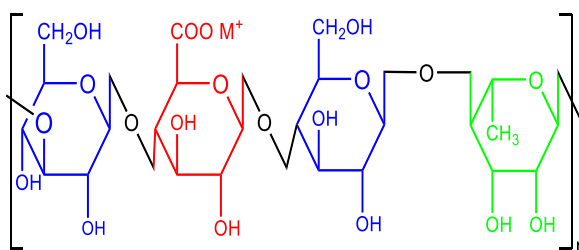


Figure 1. Chemical structure of gellan gum.

Gellan gum, utilized in solutions across a variety of molar masses, serves multiple purposes, including as a food, antioxidant activities, in drug delivery systems, and plant growth regulators [16,17].

In the literature, relevant studies have primarily explored the formulation of the Mark–Houwink equation [18], the structural and conformational properties of polysaccharides in organic solvents [19], and the impact of radiation on the molar mass-viscosity relationship [20]. However, our research specifically examines radiation-induced M - P modifications in diluted gellan within an aqueous solution, a topic that has not yet been addressed in previous studies.

This study seeks to offer scientists and engineers working with polymers and polysaccharides an efficient approach to modifying gellan in aqueous solution for targeted applications. The objectives of the study are categorized into three main areas: examining radiation degradation kinetics, establishing scaling laws, and analyzing changes in chain flexibility following modification.

2. Experimental

2.1. Materials

Gellan was supplied as commercial-grade powder by Glentham Life Sciences Ltd at UK. The Potassium Chloride (KCl) powered was supplied as Commercial-grade powder by Surechem products ltd, Needham market, Suffolk, UK.

2.2. Solution preparations

Potassium chloride, KCl, was dissolved in double-distilled water to obtain a stock solvent up to 0.1M. Gellan gum, GG, was then dissolved in the solvent to obtain a stock solution up to 0.05 g/cm³. In both dissolution proses, the mixture was gently stirred using a magnetic stirrer to ensure complete dissolution.

2.3. Viscosity measurements

Viscosity measurements were performed using a thermostated water bath (TCB-7-Viscometer Bath, 230V/50-60Hz, PSL-Rheotek) maintained at a temperature of $24.99 \pm 0.01^\circ\text{C}$. The measurements utilized an Ostwald viscometer (YUCHENGTECH) with a capillary diameter of 0.5 mm and a water flow time ranging from 100 to 150 seconds. Flow times for both the solvent and the solution were measured in triplicate, and their averages were calculated using Eq. 1[1,6]:

$$\eta_r = t / t_0, \quad \eta_{sp} = \eta_r - 1 \quad (1)$$

Here, t , t_0 , η_r , and η_s represent the solution flow time, solvent flow time, relative viscosity, and specific viscosity, respectively.

2.4. E-beam irradiation

The solution samples were irradiated using a digital linear accelerator manufactured by Elekta Infinity Company in Sweden, situated at the National Oncology Center in Benghazi, Libya. The irradiation process was conducted in an air atmosphere at room temperature, with electron energy of 6 MeV. The chosen absorbed dose ranged from 50 to 500 Gy, and changes in each sample were assessed through viscosity analysis immediately after irradiation and at various intervals.

2.5. Intrinsic viscosity and molar mass determinations

For the native and degraded 0.05 g/cm³ GG solutions, the intrinsic viscosity ($[\eta]$) was determined by the single-concentration method, using the Solomon–Ciuta equation [21]:

$$[\eta] = (2 \eta_{sp} - 2 \ln \eta_r)^{0.5} / C \quad (2)$$

The molar masses M_s of the native and degraded gellan were calculated, using Mark-Houwink equation (Eq.3) relating to intrinsic viscosity $[\eta]$ as [22,23]:

$$[\eta] = K_{[\eta]} M_r^a \quad (3)$$

where the M-H constantans of the used polymer-solvent system were given in the literature as [18]: $K_{[\eta]} = 7.48 \times 10^{-3} \text{ cm}^3 / \text{g}$ and $a = 0.91$.

2.6. Characterizations

2.6.1. Degradation kinetics

The degradation rate (k) of GL in the diluted solution was graphically obtained by using Eq.4 [10,24]:

$$1/M_D - 1/M_0 = k D/M_u \quad (4)$$

where: M_D is GL molar mass at specific radiation dose, M_0 is the initial GL molar masses, and M_u is the monomeric GL molar mass. Furthermore, the rate constant k is related to the first order lifetime (τ) as:

$$1/k = \tau \quad (5)$$

2.6.2. Scaling laws

The scaling parameters, including R_g and A_2 , were determined using calculations based on Eq.(6) and (7), respectively [1,4,13]:

$$R_g = \frac{M[\eta]}{\Phi_\theta})^{1/3}, \Phi_\theta = 3.7 \times 10^{24} \text{ mol}^{-1} \quad (6)$$

$$A_2 \approx \frac{[\eta]}{M} \quad (7)$$

Then, the scaling coefficients (ν and ν_{A2}) were respectively deduced from the scaling laws [4,13]:

$$\ln R_g = K_{Rg} + \nu \ln M_r, \quad (8)$$

$$\ln A_2 = K_{A2} + \nu_{A2} \ln M_r, \quad (9)$$

where K_{Rg} and K_{A2} are the equations proportionality constants.

2.6.3. Chain flexibility

The chain flexibility parameters under non-theta conditions, including the shape parameter (ρ_{shape}), activation energy ($E_{[\eta]}$), and solution entropy (ΔS), were determined using equations (10), (11), and (12), respectively [1,6,14]:

$$\rho_{\text{shape}} = \frac{R_g}{R_h} \quad (10)$$

$$\ln[\eta] = \ln A_{[\eta]} + \frac{E_{[\eta]}}{RT} \quad (11)$$

$$\Delta S_o + \ln \frac{\eta_r}{N_A h} = -\frac{\Delta S}{R} + \frac{\Delta H_r}{RT} \quad (12)$$

In the above equations R_h was computed from the relation:

$$R_h = \left(\frac{3[\eta]M}{10\pi N_A} \right)^{1/3} \quad (13)$$

where N_A is the Avogadro constant; $A_{[\eta]}$, R , and T are respectively the activation energy, Arrhenius-like constant, gas constant, and the temperature in Kelvin; ΔS_o , ΔS , ΔH_r , and h are the solvent entropy, solution entropy, relative enthalpy, and the Plank constant, respectively.

The equations (14), (15), and (16) were utilized to determine the characteristic ratio (C_∞), end-to-end distance (R_θ), and persistence length (l_p), respectively, to assess chain flexibility under theta conditions [1,4,5,8]:

$$C_\infty = \frac{Nb^2}{R_\theta^2} \quad (14)$$

$$R_\theta = \left(\frac{[\eta]_\theta M}{\Phi} \right)^{1/3} \quad (15)$$

$$l_p = \frac{bC_\infty}{2} \quad (16)$$

The following relationships were considered during the application of the above equations [1,25,26]:

$$N = 2M/M_u \quad (17)$$

$$\Phi \approx 2.5 \times 10^{23} \text{ mol}^{-1} \quad (18)$$

$$[\eta]_\theta = \frac{[\eta][1 - \exp(-\frac{c}{c^*})]}{\frac{0.77^3 \rho_{\text{chain}}}{c^*} - \exp(-\frac{c}{c^*})} \quad (19)$$

$$\rho_{\text{chain}} = \frac{2.5}{[\eta]} \quad (20)$$

$$C^* \approx \frac{0.77}{[\eta]} \quad (21)$$

where Φ , $[\eta]_{\theta}$, ρ_{ecu} , and C^* are known as the Flory constant, intrinsic viscosity at theta condition, chain density, and its critical concentration, respectively.

3. Results and discussion

3.1. Degradation kinetics

Figure 2 shows how EB-radiation affects gellan when it is in a solution. The observed rapid decrease indicates a strong molar mass reduction up to an absorbed dose of 200 Gy. After that point the no major reduction were seen. This behavior happens because of random chain breaks, which are likely to occur at a steady rate during the fast decline part. According to Figure 2, the rate constant was found to be a $1.03 \times 10^{-5} \text{ Gy}^{-1}$ and the lifetime was $97 \times 10^3 \text{ Gy}$.

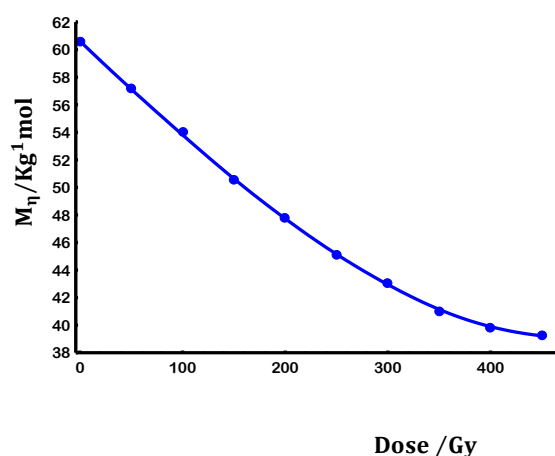


Figure 2. Progress of E-beam degraded molar mass for gellan samples at 25°C.

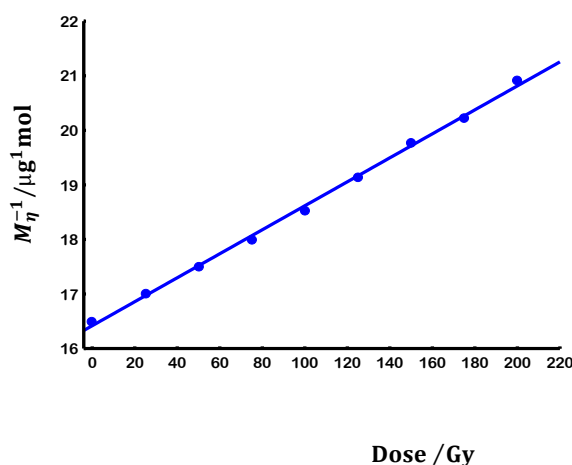


Figure 3. First order degradation law of native gellan sample by E-beam at 25°C.

3.2. Scaling laws

Similar to the degraded molar masses (M_s) shown in Figure 2, Figure 4 illustrates the effect of EB-radiation on the size parameter R_g of the polymer-solvent system. A logarithmic plot in Figure 4 was then utilized to derive the corresponding scaling law.

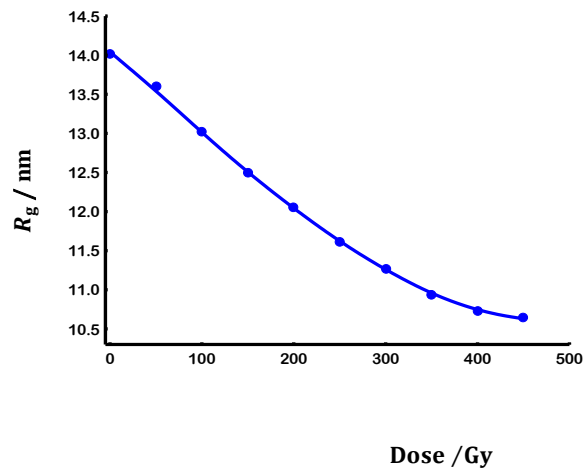


Figure 4. Progress of E-beam degraded radius of gyration for gellan samples at 25°C.

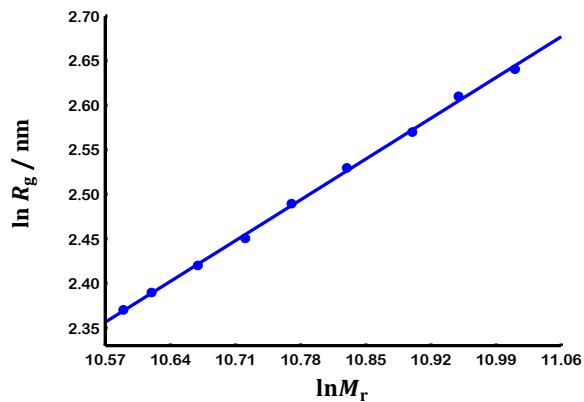


Figure 5. The logarithmic forms of radius of gyration vs molar mass for gellan samples at 25°C.

In contrast to the reduction in size observed in Figure 4, Figure 6 highlights the increase in solvation parameters A_2 caused by the EB-radiation, which was used to determine the solvation scaling law through its logarithmic representation Figure 7

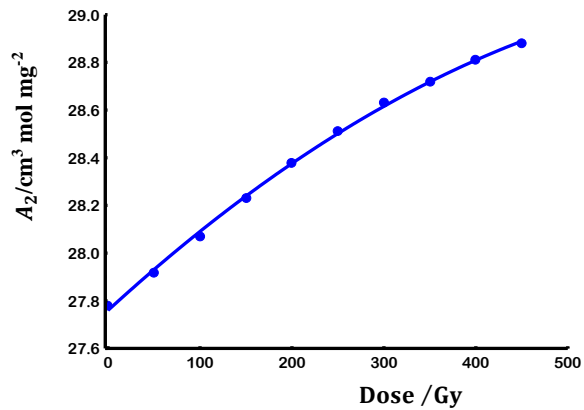


Figure 6. Progress of E-beam degraded second virial coefficient for gellan samples at 25°C.

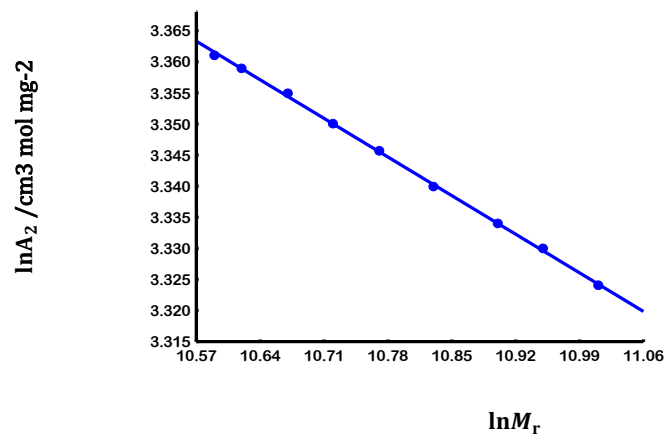


Figure 7. The logarithmic form of second virial coefficient vs molar mass for gellan samples at 25°C.

The above scaling laws offer valuable frameworks for tailoring the desired R_g and A_2 using EB-radiation. Additionally, their coefficients ν and ν_{A_2} , along with the M-H scaling coefficient a , which was calculated as $a = 3\nu - 1$ [1,4,5], were employed to predict the real perturbed chain, as summarized in Table 1.

Table 1. Scaling coefficients of gellan samples at 25°C.

Coefficient	Value
a	0.80
ν	0.62
ν_{A2}	0.15

3.3. Chain flexibility

3.3.1. Evaluation at non-theta conditions

Figures 8 and 9 illustrate Eq. 10 and 11, respectively, for large (L), medium (M), and small (S) molar masses of diluted gellan in the solvent used. These are represented by the linear plots shown in the figures.

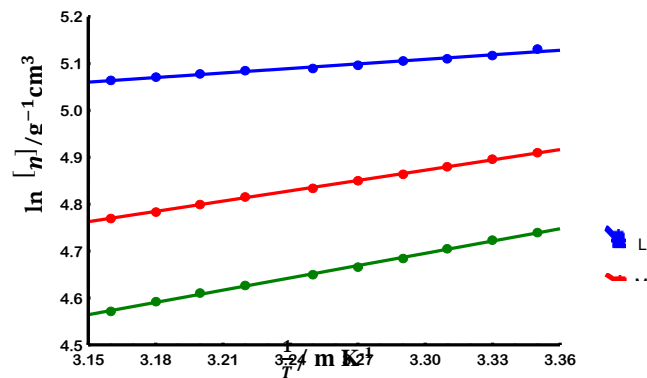


Figure 8. Arrhenius like plots of large, medium and small size for gellan samples at different temperature.

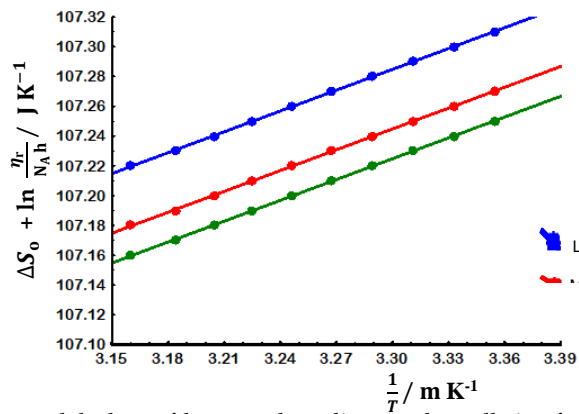


Figure 9. Kauzmann- Eyring model plots of large and medium and small size for gellan samples at different temperature.

The linear plots in Figures 8 and 9 were utilized to calculate $E_{[\eta]}$ and ΔS values, respectively. These values, along with their corresponding ρ_{shape} values, are summarized in Table 2 to assess the effect of EB radiation on them and, consequently, on gellan flexibility.

Table 2. Chain characteristics of gellan samples under non-theta conditions.

<i>M</i>	$\frac{E_{[\eta]}}{\text{kJ/mol}}$	$\frac{\Delta S}{\text{J/K mol}}$	ρ_{shape}
L	2.66	-879	1.19
M	2.16	-878	1.19
S	1.74	-877	1.19

As in Table 2, EB radiation led to a decrease in M_s and $E_{[\eta]}$ s of gellan in solution, while it increased ΔS of gellan in solution. This reduction in $E_{[\eta]}$ caused a decrease in the flexibility of the gellan chain [6,14]. Conversely, the solvent quality (SQ) was enhanced by EB radiation due to the increase in its ΔS [6]. However, the ideal random coiled structure of gellan, as defined by its ρ_{shape} , remained unaffected by EB-radiation.

3.3.2. Evaluation at theta conditions

Figures 10 and 11 illustrate the relationships between C_∞ and l_p with R_θ , which represents the chain size, for both native and degraded gellan samples. As expected, these characteristics are influenced by the gellan chain length and related molar mass M , particularly at high values of R_θ .

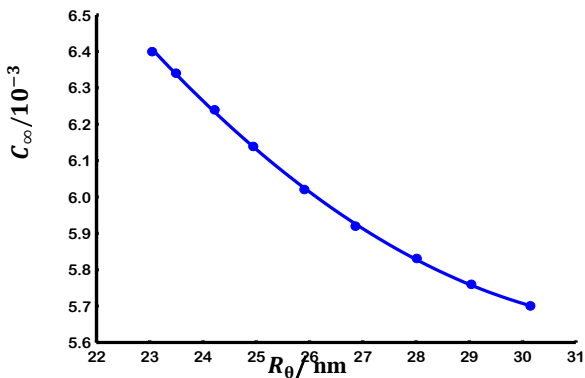


Figure 10. End to end distance vs characteristic ratio for gellan samples at 25°C.

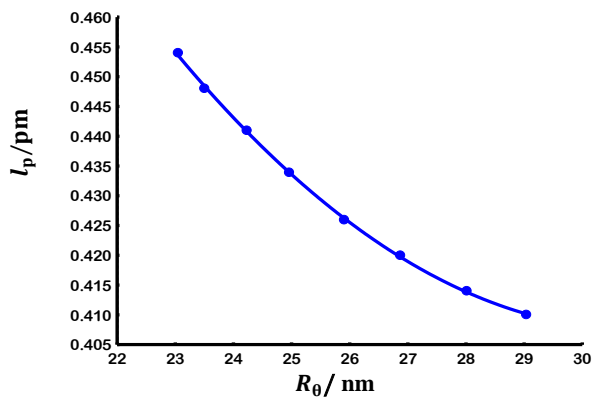


Figure 11. End to end distance vs persistence length for gellan samples at 25°C.

The M dependencies of these characteristics are summarized in Table 3. As shown in Table 3, EB radiation resulted in a reduction in M_s and R_0 of the GL samples, while increasing l_p . This increase led to a decrease in CF and an increase in SQ of the gellan samples, as discussed in section 3.3.1. Additionally, the data in Table 3 indicate no deviation from chain ideality, as reflected by C_∞ , at the molar masses listed in Table 3.

Table 3. Chain characteristics of gellan samples under theta conditions.

M	$\frac{R_0}{nm}$	$\frac{C_\infty}{10^{-3}}$	$\frac{l_p}{pm}$
L	30.15	5.69	0.40
M	25.91	6.08	0.43
S	23.05	6.40	0.45

4. Concluding remarks

- (1) Viscometry serves as an effective technique for analyzing radiation-modified gellan in diluted aqueous solutions.
- (2) Electron beam (E-beam) degradation enables precise control over the applicability of gellan solutions, by modifying the relationship between molar mass and viscosity.
- (3) Gellan scaling laws have practical significance for users, allowing them to tailor the polymer’s molar mass to achieve desired properties and vice versa.
- (4) Activation parameters, including activation energy and activation entropy, can be utilized to assess the flexibility of both native and modified gellan through relative viscosity measurements.
- (5)The flexibility characteristics of native and E-beam-degraded gellan chains, such as end-to-end distance and persistence length, can be determined using the Mark-Houwink relationship under theta conditions.

References

1. Kulicke WM, Clasen C. Viscosimetry of polymers and polyelectrolytes. Berlin: Springer; 2004.

2. W. B. Jensen, “The Origin of the Term Allotrope,” J. Chem. Educ., 2006, 83, 838-839..

3. W. Kuhn, Kolloid-Zeitschrift, 1934, 68, 2–15.

4. P. J. Flory, Principles of polymer chemistry, Cornell university press, 1953.

5. P. J. Flory, Statistical Mechanics of Chain Molecules, Hanser-Gardner, Ohio, 1989.

6. Moore WR. Viscosities of dilute polymer solutions. Progress in polymer science. 1967 Jan 1;1:1-43.

7. M. Kurata and Y. Tsunashima, in The Wiley Database of Polymer Properties, 1999.

8. R. Lapasin, Rheology of industrial polysaccharides: theory and applications, Springer Science & Business Media, 2012.

9. Li S, Xiong Q, Lai X, Li X, Wan M, Zhang J, Yan Y, Cao M, Lu L, Guan J, Zhang D. Molecular modification of polysaccharides and resulting bioactivities. *Comprehensive Reviews in Food Science and Food Safety*. **2016** Mar;15(2):237-50.
10. Al-Assaf S, Coqueret X, Zaman HM, Sen M, Ulański P, editors. *The radiation chemistry of polysaccharides*. Vienna, Austria: International Atomic Energy Agency; **2016**.
11. Hamdani AM, Wani IA, Gani A, Bhat NA, Masoodi FA. Effect of gamma irradiation on physicochemical, structural and rheological properties of plant exudate gums. *Innovative Food Science & Emerging Technologies*. **2017** Dec 1;44:74-82.
12. N. L. del Mastro, in *Radiation-Processed Polysaccharides: Emerging Roles in Agriculture*, eds. M. Naeem, T. Aftab and M. M. A. Khan, Academic Press, **2022**, pp. 91–106.
13. Krigbaum WR, Flory PJ. Statistical Mechanics of Dilute Polymer Solutions. IV. Variation of the Osmotic Second Coefficient with Molecular Weight. *Journal of the American Chemical Society*. **1953** Apr;75(8):1775-84.
14. Kauzmann W, Eyring H. The viscous flow of large molecules. *Journal of the American Chemical Society*. **1940** Nov;62(11):3113-25.
15. Kratky O, Porod G. Röntgenuntersuchung gelöster fadenmoleküle. *Recueil des Travaux Chimiques des Pays-Bas*. **1949**;68(12):1106-22.
16. Prajapati VD, Jani GK, Zala BS, Khutliwala TA. An insight into the emerging exopolysaccharide gellan gum as a novel polymer. *Carbohydrate polymers*. **2013** Apr 2;93(2):670-8.
17. Lalebeigi F, Alimohamadi A, Afarin S, Aliabadi HA, Mahdavi M, Farahbakhshpour F, Hashemiavali N, Khandani KK, Eivazzadeh-Keihan R, Maleki A. Recent advances on biomedical applications of gellan gum: A review. *Carbohydrate Polymers*. **2024** Jun 15;334:122008.
18. Drevet E, Monot F, Lecourtier J, Ballerini D, Choplin L. Influence of fermentation hydrodynamics on gellan gum physico-chemical characteristics. *Journal of fermentation and bioengineering*. **1996** Jan 1;82(3):272-6.
19. Kang D, Cai Z, Wei Y, Zhang H. Structure and chain conformation characteristics of high acyl gellan gum polysaccharide in DMSO with sodium nitrate. *Polymer*. **2017** Oct 16;128:147-58.
20. Gao M, Li H, Yang T, Li Z, Hu X, Wang Z, Jiang Y, Zhu L, Zhan X. Production of prebiotic gellan oligosaccharides based on the irradiation treatment and acid hydrolysis of gellan gum. *Carbohydrate polymers*. **2022** Mar 1;279:119007.
21. Solomon OF, Ciută IZ. Détermination de la viscosité intrinsèque de solutions de polymères par une simple détermination de la viscosité. *Journal of applied polymer science*. **1962** Nov;6(24):683-6.
22. Mark H. Über die entstehung und eigenschaften hoch polymer festkörper. In: Sanger R. editor. *Der festkörper*. Leipzig: Hirzel; **1938**. p. 65-104.
23. Houwink R. Zusammenhang zwischen viscosimetrisch und osmotisch bestimmten Polymerisationsgraden bei Hochpolymeren. *J. Prakt. Chem.* **1940**;157(1-3):15-18.
24. Şen M, Taşkın P, Güven O. Effects of polysaccharide structural parameters on radiation-induced degradation. *Hacettepe Journal of Biology and Chemistry*. **2014**;42(1):9-21.
25. Qian JW, Wang ML, Han DL, Cheng RS. A novel method for estimating unperturbed dimension $[\eta]_0$ of polymer from the measurement of its $[\eta]$ in a non-theta solvent. *European polymer journal*. **2001** Jul 1;37(7):1403-7.
26. Graessley WW. Polymer chain dimensions and the dependence of viscoelastic properties on concentration, molecular weight and solvent power. *Polymer*. **1980** Mar 1;21(3):258-62.

Disclaimer/Publisher's Note: The statements, opinions and data contained in all publications are solely those of the individual author(s) and contributor(s) and not of MDPI and/or the editor(s). MDPI and/or the editor(s) disclaim responsibility for any injury to people or property resulting from any ideas, methods, instructions or products referred to in the content.